

## **DEVELOPMENT OF SUPPORT TOOL FOR THERMAL AND LUMINOUS ENVIRONMENTAL DESIGN IN OUTDOOR AND SEMI-OUTDOOR LIVING SPACE USING NUMERICAL ANALYSIS**

Kazuaki Nakaohkubo<sup>1</sup> and Akira Hoyano<sup>1</sup>  
<sup>1</sup>Tokyo Institute of Technology

Interdisciplinary Graduate School of Science and Engineering, Tokyo Institute of Technology,  
Yokohama, Japan, nakaokubo@hy.depe.titech.ac.jp

### ABSTRACT

The purpose of this study is to develop a design support tool by combining a thermal environment simulation with a luminous environment simulation for urban outdoor and semi-outdoor living spaces. In order to evaluate thermal and luminous environments in parallel, a radiation transfer simulation algorithm with high-resolution mesh model was developed. The results of the application to an area containing membrane structure buildings confirmed that this simulation tool is capable of examining this trade-off between thermal and luminous environments.

### INTRODUCTION

In recent years, the deterioration of the thermal environment in the urban areas of Japan has resulted in an increase in heat prostration victims during the summer. One of the methods of creating a comfortable thermal environment is by blocking solar radiation with trees, eaves, or membrane roofs. While solar shading provides a comfortable thermal environment, it also creates dark spaces. Thus, in order to create a thermal and visual comfort at outdoor living space, it is important to develop a simulation tool that is capable of examining the trade-off between thermal and luminous environments when planning urban blocks and designing buildings.

Some researchers have coupled daylighting and thermal simulation for indoor environment (e.g. Franzetti et al., 2004). In order to evaluate luminous environment in outdoor space, Miguët (2002) was developed daylight simulation tool for urban and architectural spaces. And, ENVI-met (Bruse et al., 1998) is a three-dimensional microclimate model designed to simulate microscale interactions between urban surfaces, vegetation and the atmosphere in an urban environment. However, only few attempts have so far been made at coupling luminous environment simulation and thermal simulation for outdoor living space.

The thermal design tool for use in outdoor spaces is based on a heat balance simulation that was

developed by author's group (Takashi A et al., 2008). This tool allows designers to simulate the surface temperature distribution of urban blocks while taking into consideration the actual design of the urban areas, including the buildings, the landscape and surrounding vegetation. Using this thermal design tool, the mean radiant temperature (MRT) distribution of an urban outdoor living space can be calculated. However, the MRT distribution calculated by this tool only evaluates the influence of long wave radiation. Recently, materials with high solar reflectance as well as translucent materials have been in use in building construction. These materials make it possible to deteriorate thermal comfort because solar radiation is incident to human bodies. Thus, the MRT distribution should be computed including influence of not only long wave radiation but also solar radiation. Furthermore, the influence these materials have on the luminous environment needs to be clarified.

In the present study, we propose a simulation tool that can predict the horizontal illuminance distribution as well as the distribution of MRT by considering solar radiation. We developed this tool in order to evaluate luminous and thermal environments in parallel.

### DEVELOPMENT OF THE SIMULATION ALGORITHM

#### **Outline of this simulation tool**

In order to develop a practical simulation tool which don't require expert knowledge, the input and pre-processing method of this tool were developed using the features of the 3D-CAD system and the GUI. The CAD models made using above system are then transformed into a 3D-voxel mesh model that includes the calculation parameters required for thermal and luminous environment simulation. Thermal and luminous environment simulation were carried out. In the post-process of this system, the result of surface temperature distribution are visually projected onto the 3D-CAD model generated in the pre-process. And horizontal illuminance and

mean radiant temperature distribution also depict on the 3D-CAD. Figure 1 shows the flow of this simulation tool. Detailed account of the algorithm was mentioned below.

### Reproduction method for spatial geometry and material position on buildings and the ground

It was necessary to reproduce spatial geometries and material positions because these factors have an effect on the thermal radiation and luminous environments of outdoor living spaces. To accomplish this, the following steps were taken:

1. The target spatial geometry including buildings, materials used, positions and the surrounding landscape were recreated by 3D-CAD.
2. The CAD models created above were then transformed into a three-dimensional 3D-voxel mesh model that included the calculation parameters required for radiative analysis and heat transfer analysis. The voxel mesh size was set at 0.2 m in order to reproduce detailed outdoor spatial geometry (Figure 2).
3. The calculation parameters (material properties, such as optical reflectance, solar reflectance, volumetric specific heat and normal direction of the surface, etc.) were entered at each point in the 3D-voxel mesh (Figure 3).

### Weather conditions

In order to evaluate thermal environment and luminance environment in parallel, it is important to use the same weather data when calculating thermal and luminous environments. Thus, in this study, direct sunlight illumination and skylight illumination were computed multiplying the direct solar radiation and sky solar radiation by luminous efficacy which was suggested by Igawa (Norio I et al., 1999).

### Illuminance calculation method

The simulation tool developed for this study evaluates luminous environments by observing horizontal illuminance. The reference point was 1.5 meters above ground level. In order to estimate horizontal illuminance, direct illuminance and indirect illuminance needed to be calculated (Figure 4).

#### 1) Direct illuminance

##### (i) Direct sunlight illuminance

Direct sunlight illuminance was simulated by a ray-tracing method. In this method, the ray-tracing starting reference point and the tracer extends upward to the solar position. Direct sunlight illuminance was allotted to any point if the ray being traced was not

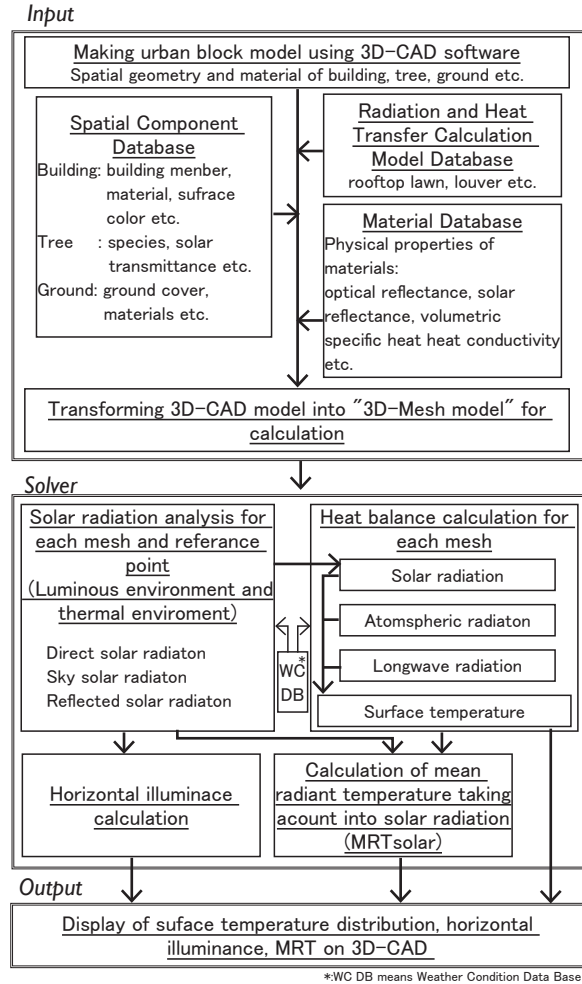


Figure.1 The flow chart of this simulation tool

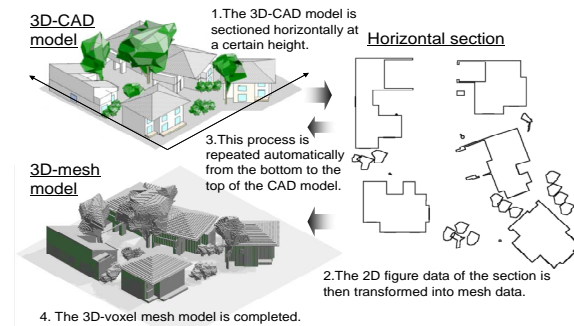


Figure.2 Schimatic diagram of the mesh model generation

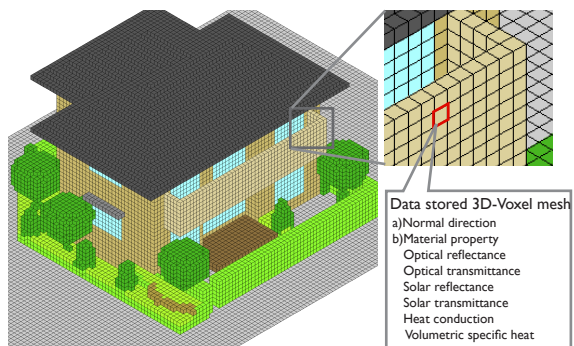


Figure.3 3D-Voxel Mesh

blocked in the calculation area.

(ii) Skylight illumination

Skylight illuminance was computed taking into account sky luminance distribution. In this study, sky luminance distribution was calculated by the All Sky Model (Norio I et al., 2004). The multi-tracing simulation calculated skylight illuminance from the reference point towards multiple hemispherical directions. The tracing direction is established in a way that allows the tracing density to have the same configuration factor (Figure 5, Formula (1)). Skylight illuminance was estimated by aggregating the sky luminance obtained at the upper boundary surface that the tracers could reach.

2) Indirect illuminance

In order to compute indirect illuminance at the reference points, it was necessary to calculate luminous emittance of buildings and ground surfaces. The calculation algorithm used was as follows:

(i) Direct sunlight illuminance and skylight illuminance on building and ground surface

Direct illuminance on buildings and ground surfaces was estimated in the same manner as direct sunlight illuminance and skylight illuminance was at the reference points discussed above. That is, direct sunlight illumination on buildings and ground surfaces was estimated by the ray-tracing method while the multi-tracing simulation computed skylight illuminance

(ii) Reflected sunlight illuminance on building and ground surface

The illuminance received by buildings and ground surfaces due to reflected sunlight that was simulated by this method included both specular reflection and isotropic diffuse reflection. Both of these reflections considered the third reflections.

Specular reflective sunlight was calculated in such a way that the tracing simulation that extends in the direction of the specular reflection was implemented, and the luminance was allotted to any point in the mesh that the tracing could reach. Diffuse reflective sunlight was estimated based on the assumption of isotropic diffuse reflection, following Lambert's cosine law, and the illuminance that a mesh receives was calculated by performing the multi-tracing simulation toward the surrounding meshes.

The method used for the multi-tracing simulation was the same as that used for the skylight illuminance estimation. In this tracing process, if a ray tracing hit a mesh that had a diffuse reflection surface, the luminance of the reflected light of the mesh was obtained. This ray tracing method was implemented for multiple directions in order to estimate the total

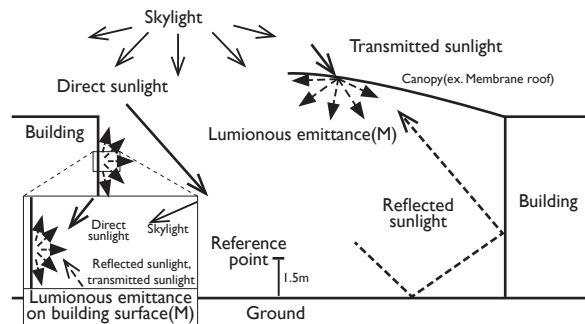
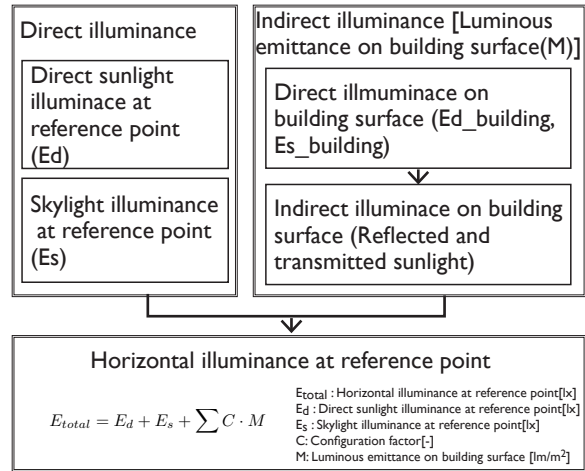
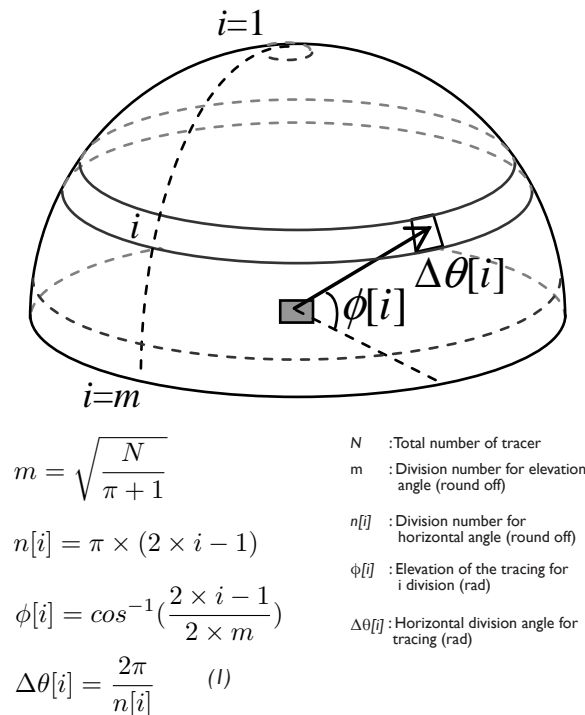


Figure.4 The flow chart of illuminance calculation



$$m = \sqrt{\frac{N}{\pi + 1}}$$

$$n[i] = \pi \times (2 \times i - 1)$$

$$\phi[i] = \cos^{-1}\left(\frac{2 \times i - 1}{2 \times m}\right)$$

$$\Delta\theta[i] = \frac{2\pi}{n[i]} \quad (1)$$

$N$  : Total number of tracer  
 $m$  : Division number for elevation angle (round off)  
 $n[i]$  : Division number for horizontal angle (round off)  
 $\phi[i]$  : Elevation of the tracing for  $i$  division (rad)  
 $\Delta\theta[i]$  : Horizontal division angle for tracing (rad)

Figure.5 Establishment of tracing directions

amount of the luminance emittance value received from the surroundings.

(iii) Transmitted sunlight illuminance on building and

ground surfaces

Transmitted sunlight was calculated by the same method as the diffuse reflective light. In this process, if a tracing hit a mesh that had a transmitted surface, the luminance of the transmitted sunlight of the mesh was obtained. The multi-tracing simulation toward the surrounding meshes was implemented in order to determine the meshes effected, which are then used to estimate the luminance from the surroundings. The multi-tracing simulation method used was basically the same as the method used for the estimation of the diffuse reflective sunlight.

### 3) Indirect illuminance at the reference point at 1.5 m

The illumination of buildings and ground surfaces was calculated by integrating the luminance that was estimated using the above method. Luminous emittance received by buildings and ground surfaces, which was computed by multiplying the illuminance by the reflectance and transmittance of the surface, was allotted to the mesh.

In the next step, indirect illuminance at the reference point was estimated by the multi-tracing simulation, which is the same method as that used to calculate skylight simulations and diffuse reflected sunlight. This tracing was implemented for multiple directions in order to estimate the total amount of indirect illumination received from the surroundings.

### Optimum number of tracers in the multi-tracing simulation

The increase in the number of tracers in the multi-tracing simulation used in estimation of skylight illuminance as well as the indirect illuminance of building and ground surfaces and the horizontal illuminance at reference plane allowed computation of more accurate results. However, the multiple factors also caused the calculation load to increase. Thus, it was important to determine the optimum number of traces for practical use. Therefore, the relationship between the number of tracers in the multi-ray-tracing simulation and the calculation accuracy using horizontal illuminance was examined.

The root mean square error (RMSE) was used as the calculation accuracy index (Formula (2)). The maximum number of tracers set as the standard for this investigation, was over 16,000.

Figure 6 shows the relationship between the number of tracers and the RMSE of the horizontal illumination for all the reference points in the calculation area. As the number of tracers increased, the value of the RMSE decreased. However, the difference in the RMSE was small when approximately 446 tracers were used. When 446 tracers were applied, the RMSE value was less than

$$RMSE = \sqrt{\frac{\sum_{i=1}^n (E_{total\_16249} - E_{total\_m})^2}{N}} \quad (2)$$

$E_{total\_16249}$  : Horizontal illuminance using the maximum number of tracer

RMSE : Calculation error index (Root Mean Square Error)

$N$  : The number of mesh

$E_{total\_m}$  : Horizontal illuminance using the each tracer number

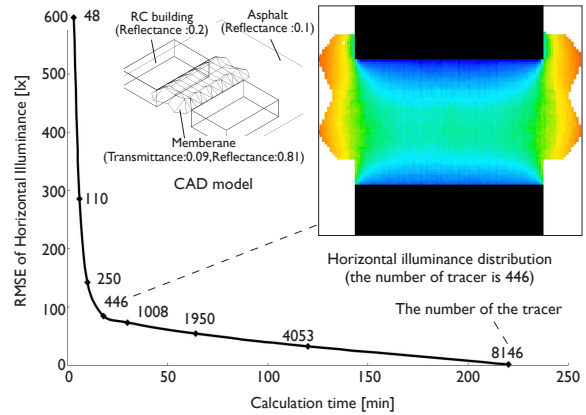


Figure.6 Relationship between the number of tracer and RMSE of illuminance

100lx. This result confirmed that optimum number of tracers for this multi-tracing simulation was more than 450.

### Calculation method for mean radiant temperature taking into account solar radiation

In this tool, mean radiant temperature taking into account solar radiation (MRT<sub>solar</sub>) was used as an index for the thermal radiant field. The calculation method was as follows.

#### 1) Human body model for calculating MRT

In order to calculate the budget of incident radiation to a human body located at an outdoor space, the following two features were considered:

1. Direct solar radiation is parallel beam.
2. Sky solar radiation, reflected solar radiation, atmospheric radiation and long wave radiation were in a radial pattern.

Therefore, in this calculation method, the following human body model was used (Figure 7).

#### (i) Human body model for direct solar radiation

The direct solar radiation area received by a human body was needed to calculate the budget of incident direct solar radiation applicable to human bodies. For this calculation method, The direct solar radiation area (formula (4)), which was suggested by Underwood (Underwood C.R. et al., 1966), was employed.



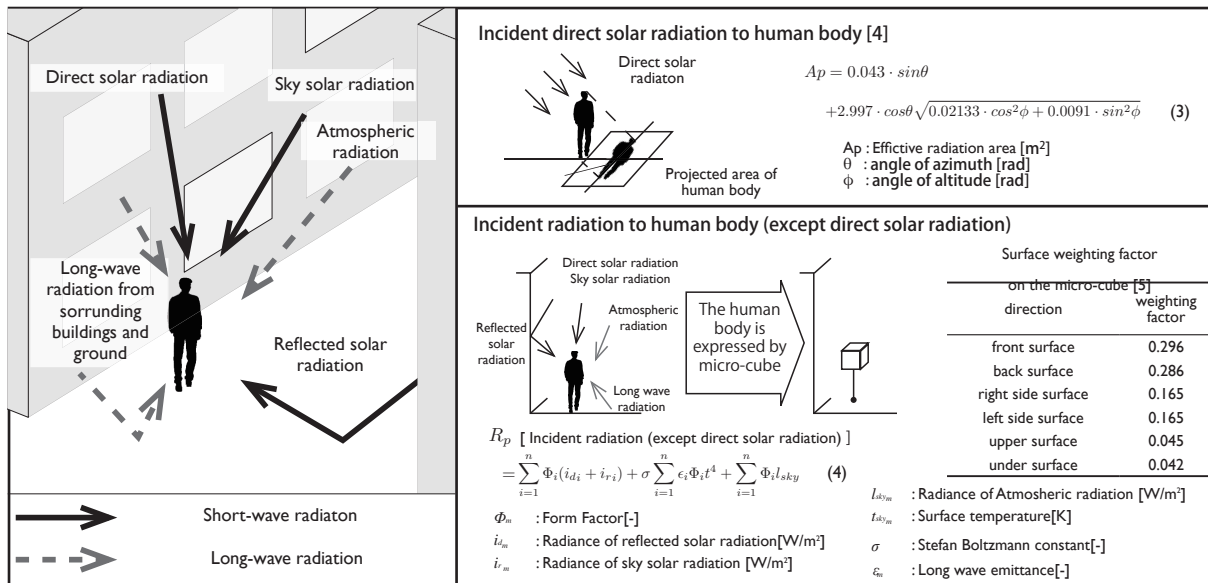


Figure 7. Human body model for calculation of incident radiation

- (ii) Human body model for sky solar radiation, reflected solar radiation, atmospheric radiation, and long wave radiation

The form factors from a human body to surrounding buildings and ground surfaces were needed in order to calculate the budget of incident radiation, except for direct solar radiation. There have been many studies that have examined the form factor from the human body to surrounding subjects. In Ozeki's method (Yoshichi O et al., 2003), which was used in our calculation, the human body was represented by a micro-cube. The relationship of form factors from a human body to objects was expressed by the surface-weighting factor on the micro-cube.

## 2) Calculation method of MRTsolar

Figure 8 shows a flow chart of this calculation method. The height of evaluation point was set at 1.5 meters.

- (i) Calculation method of solar radiation

### a) Direct solar radiation

The budget of incident solar radiation to a human body was simulated by the ray-tracing method. If the ray tracing was not interrupted by obstructions in the calculation area, the budget of direct solar radiation that the human body received was then allotted.

### b) Sky solar radiation

The budget of incident sky solar radiation was calculated by the same basic multi-tracing simulation that was used for the estimation of skylight illuminance. The sky radiance distribution was considered for computing sky solar radiation. The sky radiance distribution was estimated by All-Sky-Model-R (Norio I et al., 2004).

### c) Reflected solar radiation

The simulated reflected solar radiation included both specular reflection and isotropic diffuse reflection. The calculation method on the each micro-cube surface was the same as that used for indirect illuminance.

- (ii) Calculation method of long wave radiation

### a) Atmospheric radiation

The budget of atmospheric radiation received by the surface of micro-cube was estimated by multiplying the sky view factor and the budget of atmospheric radiation, which was calculated by Brunt's formula for unobstructed sky.

### b) Long wave radiation from the surroundings

The surface temperature distribution of buildings and ground surfaces that was needed to calculate the budget of incident long wave radiation from the surroundings into the micro-cube was simulated by Asawa's method (Takashi A et al., 2008). When calculating surface temperature, convective heat transfer was calculated under the assumption that there was no distribution of air temperature and wind velocity in the subject urban canopy and one-dimensional heat conduction was simulated. The multi-tracing simulation toward the surrounding building and ground surface meshes was implemented in order to determine the meshes used to estimate the radiant flux from the surroundings. The method of the tracing simulation was the same as that used for the estimation of diffuse reflective radiation.

- (iii) Calculation of MRT taking into account solar radiation

The incident radiation to human body was calculated by the formula (5) in Figure 8, and mean radiant

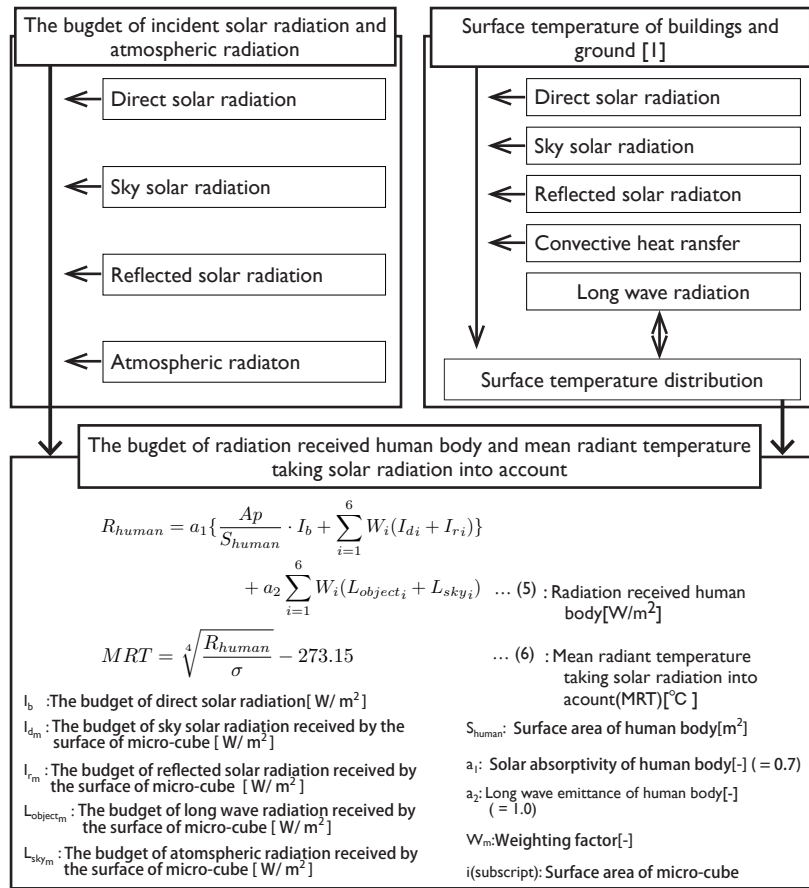


Figure 8 The flow chart of MRT calculation

temperature was then simulated by formula (6). The solar absorptivity and long wave emittance of a human body is discretionary. In this paper, solar absorptivity was set at 0.7 and long wave emittance was set at 1.0.

## SIMULATION TOOL APPLICATION

In order to confirm the applicability of this simulation tool to the purpose of thermal and luminous design of semi-outdoor spaces, it was applied to a commercial structure that consisted of semi-outdoor spaces under a membrane roof (Figure 9). The membrane was constructed of a light, solar-radiation-transmissive material. In this situation, a high-transmissive membrane roof would form a bright space, but also an uncomfortable radiation field. On the other hand, a low-transmissive membrane roof would form a dark space, but more comfortable radiation field.

Calculations were performed for two different scenarios. In the first scenario, the optical transmittance and solar transmittance of the membrane roof was set at 0.10, 0.09 (Case 1). In Case 2, the optical transmittance and solar transmittance of the membrane roof was set at 0.20, 0.18 (Table 1). Table 2 gives the reflectance of main constituent materials of building and ground. The weather

conditions used in both calculations were that of a summer day with clear skies in Tokyo (Figure 10).

### 1) Luminous environment

Figure 11 shows a horizontal illuminance distribution at 1200. The horizontal illuminance at point A under the membrane roof for Case 1 was 6500 lx. The surrounding buildings resulted in 1/15 less horizontal illuminance than the illuminance experienced at an outdoor space (10,000 lx), even though the value of membrane transmittance was 0.1. On the other hand, the horizontal illuminance at point A for Case 2 was 12,000 lx due to high transmittance level of the membrane roof.

### 2) Thermal environment

Figure 12 depicts the surface temperature distribution from viewpoint B. The difference of surface temperature at ground level between Case 1 and Case 2 was 3 °C and, the difference of surface temperature at the building wall was 2°C.

Figure 13 shows the MRTsolar distribution at a height of 1.5 m for Case 1 and Case 2. The MRTsolar condition under the membrane roof for Case 1 was 40°C, which is approximately 25°C lower than that in areas exposed to direct solar radiation. On the other hand, the MRTsolar condition under the membrane

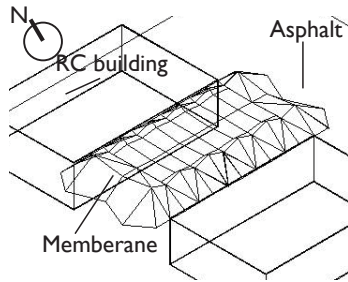


Figure 9 Calculation model

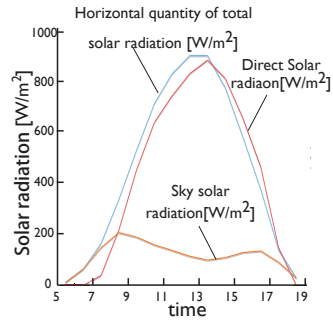


Figure 10 Weather condition

Table 1 Material property of Membrane

	CASE1	CASE2
Optical Reflectance	0.74	0.63
Optical Transmittance	0.09	0.18
Solar Reflectance	0.83	0.74
Solar Transmittance	0.10	0.20

Table 2 Material property of building

	Reflectance
Building	0.20
ground	0.10

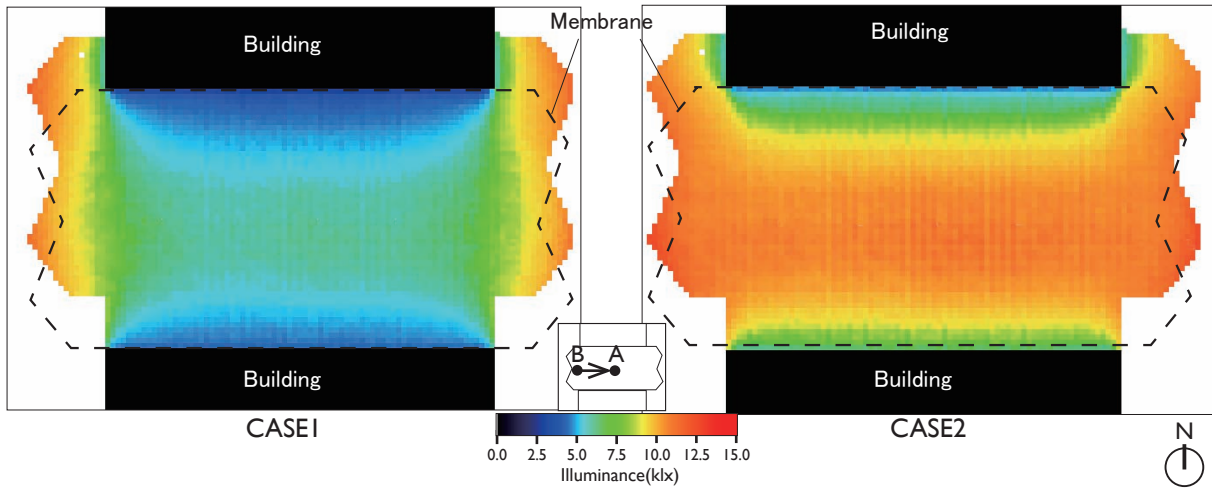


Figure 11. Horizontal Illuminance distribution at 12:00

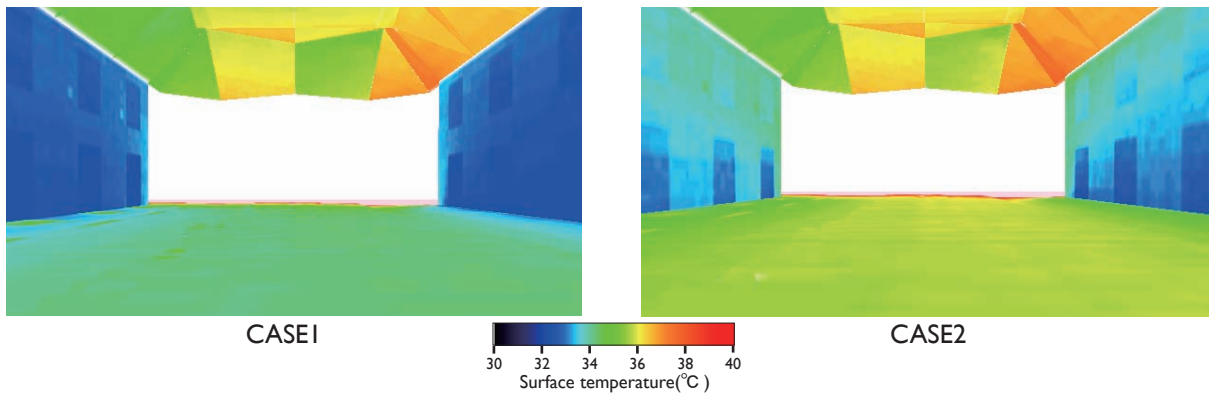


Figure 12. Surface temperature distribution from view point of B at 12:00

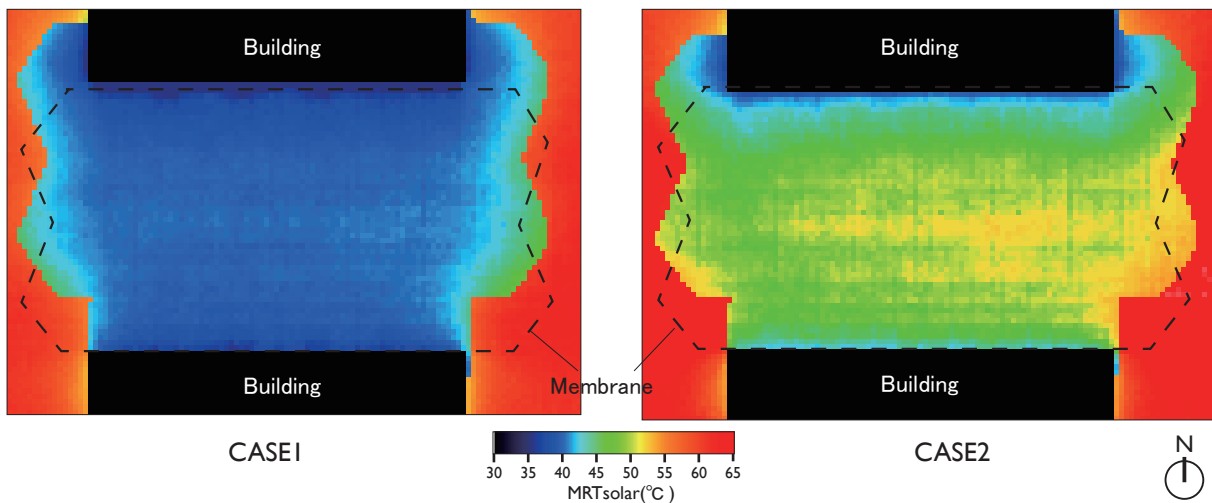


Figure 13. MRTsolar distribution at 12:00

roof for Case 2 was approximately 8°C higher than that for Case 1 due to the high solar transmittance of the membrane roof for Case 2.

These results revealed that the tool was capable of simulating the effects of building shapes and materials on the horizontal illuminance and MRTsolar distribution, and could be used to study the trade-off between luminous and thermal environments in practical semi-outdoor designs.

### CONCLUSIONS

In this paper, we described a simulation tool that is capable of predicting the horizontal illuminance and mean radiant temperature by taking into account solar radiation at outdoor and semi-outdoor living space. In order to allow consideration of detailed outdoor spatial geometry as well as material positions and types, a radiation model algorithm with a high-resolution mesh model was developed and a method of multi-tracing simulations for horizontal illuminance was examined.

The results of applying this tool in a semi-outdoor space revealed that it was capable of simulating the effects of building shapes and materials on the horizontal illuminance as well as the MRTsolar distribution, and that it could be used to study the trade-off between luminous and thermal environments in parallel.

When evaluating luminous and thermal environments in the the indoor space, objects existing in outdoor and semi-outdoor, such as trees standing beside

window, influence indoor thermal and visual comfort. Thus, In future work, a passive design tool will be developed that will be capable of evaluating the luminous and thermal environments in indoor space by combined with this simulation tool.

### REFERENCES

- Christelle Franzetti, Gilles Fraisse, Gilbert Achard, 2004. *Energy and Buildings* Volume 36, Issue 2, pp.117-126
- Francis Miguet, Dominique Groleau, 2002. *Building and Environment*, Volume 37, Issue 8-9, pp.833-843
- Bruse Michael, Fleer Heribert, 1998. *Environmental Modeling and Software*, Volume 13, pp.373-384
- Takashi Asawa , Akira Hoyano, Kazuaki Nakaohkubo, 2008. *Building and Environment*, Volume 43, Issue 12, pp.2112-2123
- Norio Igawa , Sachiyo Shimasaki, Hiroshi Nakamura, 1999. *J. Environ. Eng., AIJ*, No. 526, pp.17-24
- Norio Igawa, Yasuko Koga, Tomoko Matsuzawa, Nakamura Hirohi, 2004. *Solar Energy* Volume 77, Issue 2, pp.137-157
- Underwood C.R. and Ward E.J.: *The solar radiation area of man*, *ERGONOMICS*, vol. 9, No. 2, pp. 155-168.1966
- Yoshiichi Ozeki, Tetsuya Hiramatsu, Shin-ichi Tanabe, 2003. *J. Environ. Eng., AIJ*, No. 566, pp. 47-50